Neuronal calcium sensor-1 binds to regulated secretory organelles and functions in basal and stimulated exocytosis in PC12 cells

Bethe A. Scalettar[1,*], Patrizia Rosa[2], Elena Taverna[2], Maura Francolini[2], Takashi Tsuboi[3], Susumu Terakawa[3], Schuichi Koizumi[4], John Roder[5] and Andreas Jeromin[5]

[1]Department of Physics, Lewis and Clark College, Portland, OR 97219, USA
[2]CNR-Cellular and Molecular Pharmacology Center, Department of Pharmacology, Via Vanvitelli 32, Milan, Italy
[3]Photon Medical Research Center, Hamamatsu University School of Medicine, Hamamatsu 431-3192, Japan
[4]Division of Pharmacology, National Institute of Health Sciences, Tokyo 158-8501, Japan
[5]Samuel Lunenfeld Research Institute, Mount Sinai Hospital, Toronto, M5G 1X5 Canada
*Author for correspondence (e-mail: bethe@lclark.edu)

Accepted 5 March 2002
Journal of Cell Science 115, 2399-2412 (2002)

Summary

Neuronal calcium sensor-1 (NCS-1) and its non-mammalian homologue, frequenin, have been implicated in a spectrum of cellular processes, including regulation of stimulated exocytosis of synaptic vesicles and secretory granules (SGs) in neurons and neuroendocrine cells and regulation of phosphatidylinositol 4-kinase beta activity in yeast. However, apart from these intriguing putative functions, NCS-1 and frequenin are relatively poorly understood. Here, the distribution, dynamics and function of NCS-1 were studied using PC12 cells that stably express NCS-1-EYFP (NCS-1 fused to enhanced yellow fluorescent protein) or that stably overexpress NCS-1. Fluorescence and electron microscopies show that NCS-1-EYFP is absent from SGs but is present on small clear organelles, some of which are just below the plasma membrane. Total internal reflection fluorescence microscopy shows that NCS-1-EYFP is associated with synaptic-like microvesicles (SLMVs) in growth cones. Overexpression studies show that NCS-1 enhances exocytosis of synaptotagmin-labeled regulated secretory organelles (RSOs) under basal conditions and during stimulation by UTP. Significantly, these studies implicate NCS-1 in the enhancement of both basal and stimulated phosphoinositide-dependent exocytosis of RSOs in PC12 cells, and they show that NCS-1 is distributed strategically to interact with putative targets on the plasma membrane and on SLMVs. These studies also reveal that SLMVs undergo both fast directed motion and highly hindered diffusive motion in growth cones, suggesting that cytoskeletal constituents can both facilitate and hinder SLMV motion. These results also reveal interesting similarities and differences between transport organelles in differentiated neuroendocrine cells and neurons.

Movies available on-line

Key words: GFP, PtdIns(4,5)P_2, Synaptophysin, Frequenin, Synaptotagmin

Introduction

Neurons and neuroendocrine cells possess two exocytosis pathways: constitutive and regulated (Burgess and Kelly, 1987). The constitutive pathway supports the continuous delivery of plasma membrane proteins to the cell surface and the release of soluble proteins into the extracellular space (Halban and Irminger, 1994). By contrast, the regulated pathway supports the intracellular storage of proteins or nonpeptide neurotransmitters in two major types of regulated secretory organelles (RSOs) until release of organelle contents is triggered by a stimulus, such as an increase in intracellular Ca^{2+} levels (Scheller and Hall, 1992; Huttner et al., 1995; Bennett, 1997). These two types of RSOs are known as secretory granules (SGs) and either synaptic vesicles (SVs) in neurons or synaptic-like microvesicles (SLMVs) in neuroendocrine cells (Cutler and Cramer, 1990; De Camilli and Jahn, 1990; Halban and Irminger, 1994; Huttner et al., 1995).

Some of the molecules that play a central role in RSO targeting and exocytosis have been identified recently. These molecules include SNARE proteins, which mediate vesicle fusion with target membranes, and phosphoinositide lipids, which influence processes ranging from Ca^{2+} release from intracellular stores to organization of the cytoskeleton (Rothman, 1994; Martin, 1998). However, despite this progress, many of the molecules that participate in exocytosis are poorly understood.

Neuronal Ca^{2+} sensor-1 (NCS-1) and its nonmammalian homologue, frequenin, are pertinent examples of proteins that clearly play a role in regulated exocytosis but are otherwise relatively poorly understood (Burgoyne and Weiss, 2001). For example, overexpressed frequenin enhances stimulated neurotransmitter release in *Drosophila*, and overexpressed NCS-1 enhances stimulated hormone release in PC12 cells (Pongs et al., 1993; McFerran et al., 1998). However, despite these results, the function(s) of NCS-1/frequenin remains in many respects a mystery. Among other things, it is unclear whether these proteins enhance both basal and stimulated exocytosis or just stimulate exocytosis (Rivosecchi et al., 1994; Olafsson et al., 1995; McFerran et al., 1998; Chen et al., 2001).

The molecular basis of NCS-1 function also remains largely elusive. NCS-1 was originally implicated in the regulation of calmodulin-dependent enzymes (Schaad et al., 1996), but more recently it has been implicated in the regulation of other proteins. For example, NCS-1/frequenin stimulates the activity of phosphatidylinositol 4-kinase beta (PtdIns 4-kinase beta) in yeast and in COS-7 cells, suggesting that NCS-1 replenishes with phosphoinositides at sites of exocytosis (Hendricks et al., 1999; Meyer and York, 1999; Zhao et al., 2001). In addition, a number of diversely distributed but poorly characterized putative 'targets' for NCS-1 have been identified on the basis of binding of NCS-1 to proteins in the cytosolic fractions and chromaffin granule and microsomal membrane fractions of the adrenal medulla (McFerran et al., 1999).

The subcellular distribution and transport of NCS-1 also are not fully understood. Distribution and transport, like function, have been a focus of attention and interest, because NCS-1 may have a diversely distributed set of targets and multiple sites of action (Nef et al., 1995; McFerran et al., 1999; Meyer and York, 1999; Nakamura et al., 2001; Zhao et al., 2001). NCS-1 exists in myristoylated and non-myristoylated forms, and myristoylated NCS-1 binds to membranes (Hendricks et al., 1999; McFerran et al., 1999). Moreover, it has been suggested that myristoylation and membrane binding are important for NCS-1–target interactions, particularly involving PtdIns 4-kinase beta (Zhao et al., 2001). Unfortunately, little is known about NCS-1's interaction with specific subcellular membranes or about the transport of NCS-1 to putative sites of action.

Here we have addressed important, unresolved issues surrounding NCS-1 using stably transfected PC12 cells that express a hybrid protein, NCS-1-EYFP, consisting of NCS-1 fused to enhanced yellow fluorescent protein (EYFP), and stably transfected PC12 cells that overexpress NCS-1. Cells expressing the hybrid were used to study distribution and dynamics at high resolution, thereby elucidating NCS-1's potential sites of action, extent of colocalization with putative targets and binding to subcellular membranes. Cells overexpressing NCS-1 were used to study function. Our results show that NCS-1-EYFP binds to clear organelles, some of which are just below the plasma membrane, and to SLMVs in growth cones but not to SGs. Our results also show that NCS-1 overexpression enhances RSO exocytosis under basal conditions and during stimulation by UTP. Significantly, these results implicate NCS-1 in the enhancement of both basal and stimulated, phosphoinositide-dependent RSO exocytosis, and they show that NCS-1 is distributed strategically to interact with prominent putative targets on the plasma membrane and on SLMVs (Nef et al., 1995; Hendricks et al., 1999; Meyer and York, 1999). Our data also reveal novel attributes of SLMV dynamics in growth cones and interesting similarities and differences between protein trafficking in neuroendocrine cells and neurons.

Materials and Methods

Generation of transfected cells

Stably transfected cells expressing NCS-1-EYFP were used to visualize the distribution and dynamics of NCS-1. NCS-1 distribution is complex and therefore is easier to visualize using stably transfected cells that do not express fusion proteins too heavily.

Stably transfected cells expressing NCS-1 were used to study the function of NCS-1. These cells express the unmodified protein approximately six times more heavily than wild-type or 'vector control' cells (S.K., unpublished). Vector control cells contain the vector transfected into overexpressing cells without the NCS-1 cDNA.

To establish cell lines stably expressing NCS-1-EYFP, PC12 cells were transfected with DNA coding for this recombinant protein and selected for neomycin resistance. NCS-1 cDNA with appropriate restriction sites was amplified by PCR and subcloned into pEYFP-N1 (Clontech Laboratories, Palo Alto, CA). Several clones were established, and clone A3, expressing remarkable levels of yellow fluorescence in a large percentage of cells, was selected for further experiments. Cell lines stably overexpressing NCS-1 or stably containing the vector control were generated similarly.

Transiently transfected cells expressing synaptophysin-EGFP were used to visualize synaptophysin. DNA coding for this protein was generated using rat synaptophysin DNA that was amplified by PCR and fused in frame to the N-terminus of EGFP via a short linker. The synaptophysin-EGFP construct was subcloned into pcDNA3 (Invitrogen, Carlsbad, CA).

Wild-type PC12 cells were transiently transfected with DNA coding for synaptophysin-EGFP, as described previously (Lochner et al., 1998).

Antibodies

Antibodies against NCS-1 and the SG protein secretogranin II (SgII) were described previously (Lochner et al., 1998; Calegari et al., 1999; Werle et al., 2000). Antibodies against the Na/K ATPase and the luminal domain of the RSO membrane protein synaptotagmin I were kindly provided by Grazia Pietrini and Michela Matteoli, respectively (University of Milan, Italy). Antibodies against synaptophysin were obtained from Boehringer Mannheim (Ingelheim, Germany).

Isolation of total membrane and cytosolic fractions

To compare the distributions of endogenous NCS-1 and NCS-1-EYFP in total membrane and cytosolic fractions from wild-type and stably transfected PC12 cells, postnuclear supernatants (PNSs) were prepared from each cell line. Briefly, cells were homogenized in buffer containing 0.25 M sucrose, 1 mM $Mg(CH_3COO)_2$ and 10 mM HEPES that was supplemented with 10 μg/ml aprotinin and 2 μg/ml pepstatin A to inhibit protease activity. PNSs were prepared from the total homogenates by centrifuging at 800 ***g*** for 10 minutes. Each PNS was then centrifuged at 80,000 ***g*** for 20 minutes to separate the supernatant containing the cytosol from the pellet containing all membrane-bound organelles. The pellets were resuspended in the starting volume. 20 μL of the total membrane and cytosolic fractions were separated by electrophoresis, electroblotted to nitrocellulose and probed with antibodies as described previously (Rowe et al., 1999).

Isolation of organelle fractions

To compare the distributions of NCS-1 and NCS-1-EYFP in different organelles, total membrane fractions obtained from wild type and stably transfected PC12 cells were subjected to velocity and equilibrium centrifugation, as described previously (Tooze and Huttner, 1990; Passafaro et al., 1996). Specifically, PNSs were prepared from each cell line and centrifuged as described above. In each case, the cytosol was collected, and the pellets containing all membranes were resuspended in homogenization buffer, loaded on the top of a gradient ranging from 0.3-1.2 M sucrose and centrifuged at 110,000 ***g*** for 30 minutes (velocity gradient). 12 fractions of 1 ml each were collected from the top of the velocity gradient. 300 μL of each of fractions 4-8 were pooled, loaded on a second gradient ranging from 1.1-2.0 M sucrose and centrifuged at 110,000 ***g*** for 18 hours (equilibrium gradient). 12 fractions of 1 ml each were collected from

the equilibrium gradient. 300 μL aliquots of each fraction from both gradients were analyzed by western blotting.

The distributions of NCS-1, NCS-1-EYFP, synaptophysin and SgII in equilibrium gradient fractions were quantified by measuring band density after immunoblotting. Autoradiograms were acquired using an ARCUS II scanner (Agfa-Gevaert N.V., Mortsel, Germany), and band density was quantified using the NIH Image program 1.61 (National Technical Information Service, Springfield, VA). Results were expressed in arbitrary units.

Preparation of cells for fluorescence microscopy

In preparation for fluorescence microscopy, PC12 cells were plated onto cover slips, as described previously (Lochner et al., 1998). In most cases, cells were induced to differentiate with 50 ng/ml nerve growth factor (Life Technologies, Gaithersburg, MD).

Electrical stimulation

In studies of electrically induced exocytosis, PC12 cells expressing NCS-1-EYFP were stimulated with one current pulse (1-2 μA in amplitude and 1 millisecond in duration) applied through a micropipette (0.5-1.0 μm in diameter) attached to the cell surface, essentially as described previously (Manivannan and Terakawa, 1994). Electrical stimulation was applied to the cell body, but the induction of exocytosis was independent of the site of application of electrical stimulation.

Immunostaining and endosomal staining

To compare the distributions of endogenous synaptophysin (or endogenous SgII) and NCS-1-EYFP, stably transfected cells were immunostained either with anti-synaptophysin or anti-SgII antibodies, as described previously (Lochner et al., 1998).

To determine whether the organelles containing hybrid proteins were endosomes, transfected PC12 cells were incubated with 0.1-5.0 mg/ml TRITC- or Texas-Red-labeled dextran (Sigma Chemicals, St Louis, MO) for times ranging from 2 to 120 minutes; a range of incubation times was used to ensure labeling of early and late endosomes. We also tested for colocalization with early endosomes by staining transfected cells with an anti-transferrin receptor antibody (Zymed, San Francisco, CA).

Uptake of synaptotagmin I

To determine the effect of NCS-1 overexpression on basal RSO exocytosis, living PC12 cells containing the vector control and living PC12 cells overexpressing NCS-1 were incubated under identical conditions, with an antibody to the luminal domain of synaptotagmin I, as described previously (Coco et al., 1998). Briefly, cells were incubated with antibody for 15 or 45 minutes at 37°C and then were rinsed three times in PBS at room temperature. After this, cells were fixed and stained with a Cy3-conjugated secondary antibody. This protocol primarily monitors overexpression-induced changes in RSO exocytosis, which are manifest in changes in uptake of synaptotagmin after its exposure at the cell surface following exocytosis (Matteoli et al., 1992).

To determine the effect of NCS-1 overexpression on UTP stimulated (phosphoinositide-dependent) exocytosis, cells were treated with the anti-synaptotagmin I antibody during a 15 minute incubation with 10 or 100 μM UTP. Cells then were fixed and stained as described above.

Electron microscopy

Immunoelectron microscopy was performed essentially as described previously (Calegari et al., 1999). PC12 cells expressing NCS-1-EYFP were fixed for 10 minutes at 4°C in buffer containing 4% paraformaldehyde and 0.25% glutaraldehyde, scraped from dishes and centrifuged. Pellets containing the cells were fixed for an additional 10 minutes at 4°C. Small pieces of the pellets were infiltrated with 2.3 M sucrose in PBS, mounted and frozen in liquid nitrogen. Ultra-thin frozen sections were collected on Formvar-coated nickel grids and then were immunolabeled with anti-NCS-1 primary antibodies and secondary antibodies conjugated to 12 nm colloidal gold (Jackson ImmunoResearch Laboratories, Inc., West Grove, PA). Finally, sections were fixed, counterstained, dehydrated and embedded in LRW resin (Polysciences Inc., Warrington, PA). Grids were examined with a Philips CM 100 electron microscope. Specificity of staining was verified with controls that involved leaving out the primary antibody or incubating sections with normal rabbit IgG.

The immunoelectron microscopy data were analyzed morphometrically by digitizing images using an Arcus II scanner and then determining the density of gold particles using the analysis program Image 1.61. The density of gold particles, expressed as the number of particles per μm^2 of the different organelle areas, was analyzed over 30 μm^2, and 12 micrographs were used for quantification.

Fluorescence microscopy

Fluorescence images were collected on a DeltaVision wide-field optical-sectioning microscope system (Applied Precision Inc., Issaquah, WA) or a BioRad Radiance 2000 laser scanning microscope (BioRad, Hercules, CA).

The methodology of image acquisition depended on the type of image collected. Time-lapse images of living cells were generated by taking images of the same focal plane every few seconds. Wide-field images of fixed cells were generated by optically sectioning cells in 0.2 μm increments. Wide-field images were deblurred to improve image clarity and to facilitate tracking of vesicles (Scalettar et al., 1996).

Total internal reflection fluorescence microscopy

Total internal reflection fluorescence microscopy (TIRFM) was used preferentially to detect hybrid proteins that were close to the plasma membrane (Axelrod, 1989). Specifically, this technique was used to study organelle dynamics and exocytosis in ~30 PC12 cells expressing NCS-1-EYFP.

Evanescent excitation was achieved using prismless TIRFM (Axelrod, 1989; Tsuboi et al., 2000; Tsuboi et al., 2001). The optical configuration used here generated an evanescent electric field that selectively excited fluorescence from hybrid proteins that were within ~70 nm of the fluid-glass interface. This fluorescence was recorded at 33 millisecond intervals with an image intensified CCD camera (Imagista, Tokyo, Japan) combined with an additional image intensifier (VideoScope, Sterling, VA).

Data analysis

The TIRFM data were analyzed by drawing circles of diameter 707 nm and circular annuli with inner and outer diameters of 707 nm and 1767 nm around puncta and quantifying the temporal dependence of the average fluorescence in these circles and annuli (Zenisek et al., 2000).

Vesicles were assumed to have undergone stimulation-induced exocytosis if the data generated using the circles and annuli exhibited two trends (Zenisek et al., 2000). First, the average fluorescence signal originating in the circle surrounding the vesicle had to increase and then to decrease following electrical stimulation. Because the evanescent electric field becomes more intense with decreasing distance from the plasma membrane, this first trend indicates that the

vesicle initially moved closer to the membrane, reflecting transport and/or vesicle flattening onto the membrane and then either retreated from the membrane or fused with the membrane permitting fluorophores to spread out of the circle (Zenisek et al., 2000). Second, the average fluorescence signal originating in the annulus surrounding the vesicle had to increase and then to decrease following electrical stimulation. Because fusion, but not retreat, will cause fluorescence to spread into the annulus, this second trend indicates that the vesicle underwent fusion.

Vesicle dynamics was characterized qualitatively by tracking and computing trajectories. Specifically, coordinates of individual vesicles were tabulated as a function of time and converted into trajectories, as described previously (Abney et al., 1999).

Vesicle motion was characterized quantitatively by computing the mean-squared displacement, $\langle r^2 \rangle$, of vesicles as a function of time, t, and fitting to a model that describes 'diffusive' and 'directed' motion as follows (Saxton and Jacobson, 1997; Abney et al., 1999):

$$\langle r^2(t) \rangle = 4Dt + v^2t^2 \quad (1)$$

Here, r is displacement, D is the diffusion coefficient and v is speed; brackets $\langle\rangle$ denote averaging, which was performed using a 'single-particle tracking' algorithm that is well suited to extracting the correct underlying dynamics (e.g. diffusive or directed) when motion is monitored for only a finite time (Abney et al., 1999). In Equation 1, diffusive motion produces a linear relationship between $\langle r^2 \rangle$ and t, whereas directed motion produces a linear relationship between $\langle r^2 \rangle^{1/2}$ and t. Ds and vs were computed from fits to Equation 1, as described previously (Abney et al., 1999).

Results

Distributions of NCS-1 and NCS-1-EYFP

We studied and compared the distributions of NCS-1 and NCS-1-EYFP in PC12 cells using subcellular fractionation and fluorescence and electron microscopy.

We first mapped and compared distribution in undifferentiated PC12 cells using subcellular fractionation techniques. Fig. 1A shows the distributions of endogenous NCS-1 and NCS-1-EYFP in cytosolic and total membrane fractions obtained from a well characterized wild-type PC12 cell clone (PC12-251) and a stably transfected PC12 cell clone (PC12-A3). In wild-type cells, endogenous NCS-1 was detected in both the cytosolic and total membrane fractions (McFerran et al., 1998). In transfected cells, NCS-1-EYFP was more highly expressed than endogenous NCS-1, and both proteins again were detected in both the cytosolic and total membrane fractions.

Fig. 1B,C compares the distributions of NCS-1, NCS-1-EYFP, synaptophysin and SgII in the various organelle-bound compartments of undifferentiated cells. To obtain these data, PNSs obtained from undifferentiated wild-type cells (left panels) or transfected cells (right panels) were centrifuged at high speed to separate membrane-bound organelles from the cytosol. The pellets containing the organelles were resuspended, and the organelles were separated using two different sucrose gradients (velocity and equilibrium) that

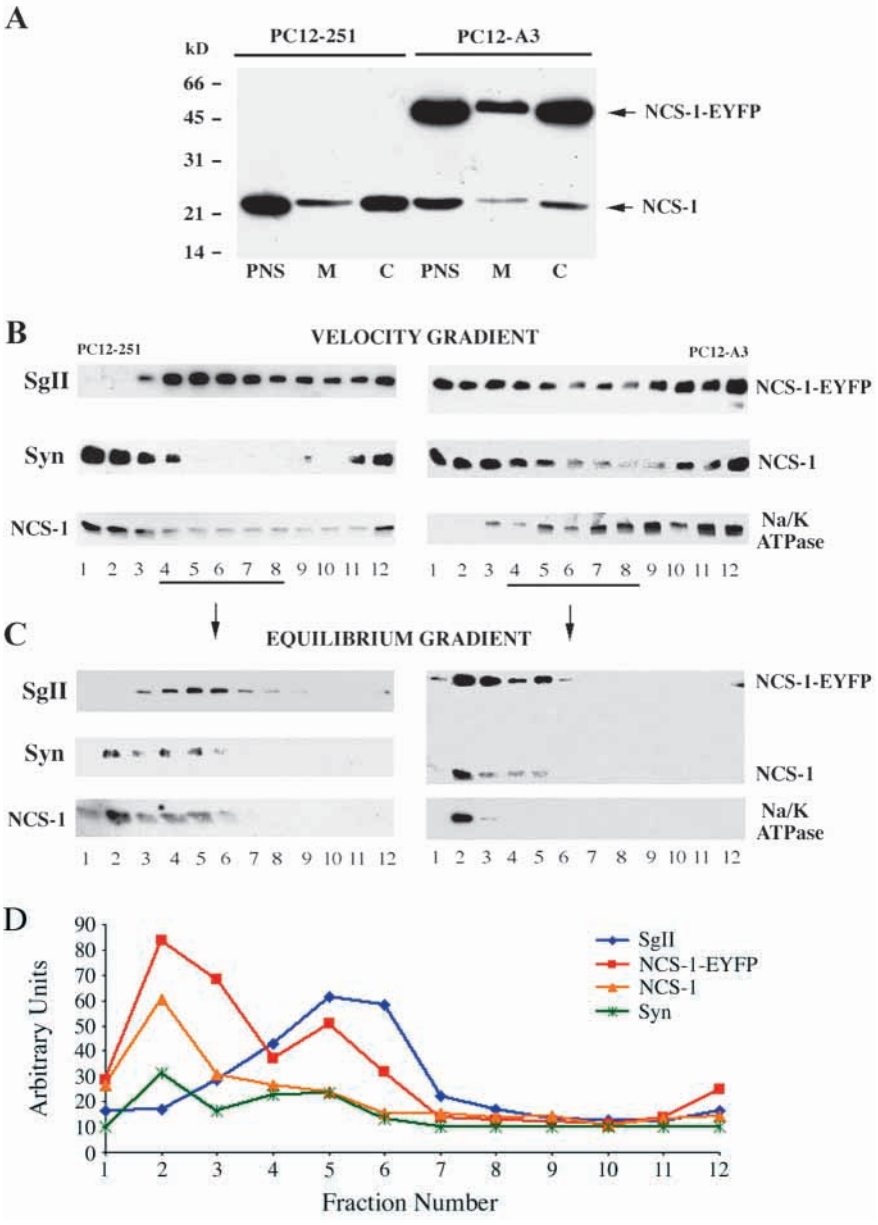

Fig. 1. Western blots (A) showing the distributions of NCS-1-EYFP and endogenous NCS-1 in postnuclear supernatants (PNS), total membrane fractions (M) and cytosolic fractions (C) obtained from wild-type and stably transfected PC12 cells. Western blots (B,C) showing the distributions of NCS-1-EYFP, endogenous NCS-1, synaptophysin (Syn) and SgII in fractions collected after (B) velocity gradient centrifugation of PNSs and (C) equilibrium gradient centrifugation of fractions 4-8 from the velocity gradient. The blots also show the distribution of the Na/K ATPase. Quantitative data (D) showing the distributions of NCS-1-EYFP, endogenous NCS-1, synaptophysin and SgII in fractions collected from the equilibrium gradient. Data were obtained using the NCS-1-EYFP band in the right panel of (C) and the NCS-1, synaptophysin and SgII bands in the left panel of (C).

produce good separation of SGs, SLMVs and other organelles (Tooze and Huttner, 1990; Passafaro et al., 1996). Fig. 1B shows protein distribution in fractions from the velocity gradients, which separate organelles on the basis of their size. Synaptophysin was enriched in the lightest fractions (1-4), which contain SLMVs, whereas SgII was present in large part in the middle fractions (4-8), which are enriched in SGs (Regnier-Vigouroux et al., 1991; Passafaro et al., 1996). In contrast, NCS-1 and NCS-1-EYFP were present in a broader spectrum of fractions. Specifically, these proteins were most prevalent in the lightest fractions (1-4) enriched in synaptophysin, but they were also present in the middle and heaviest fractions together with the SG marker SgII and the plasma membrane-marker Na/K ATPase. The visualization of these aspects of endogenous NCS-1 distribution in transfected cells required long exposure of the blots.

The results from the velocity gradient showed that some synaptophysin, Na/K ATPase, NCS-1 and NCS-1-EYFP were present in SG-containing fractions enriched in SgII. However, the SG-containing fractions from the velocity gradients probably contain both SGs and other organelles of a similar size. Thus, aliquots of the SG-containing fractions (4-8) were pooled and loaded onto an equilibrium gradient, which separates organelles on the basis of their density to achieve a better separation of SGs from other organelles. Fig. 1C,D shows that NCS-1 and NCS-1-EYFP were present mainly in the lightest fractions (2-5) from the second gradient and that their distributions again were very similar to that of synaptophysin, suggesting that NCS-1 is present on SLMVs. Fig. 1C,D also shows that NCS-1 and NCS-1-EYFP were present, at a low level, in fractions enriched in SgII, suggesting that only a very small amount of NCS-1, if any, resides on the membrane of SGs of PC12 cells (McFerran et al., 1998).

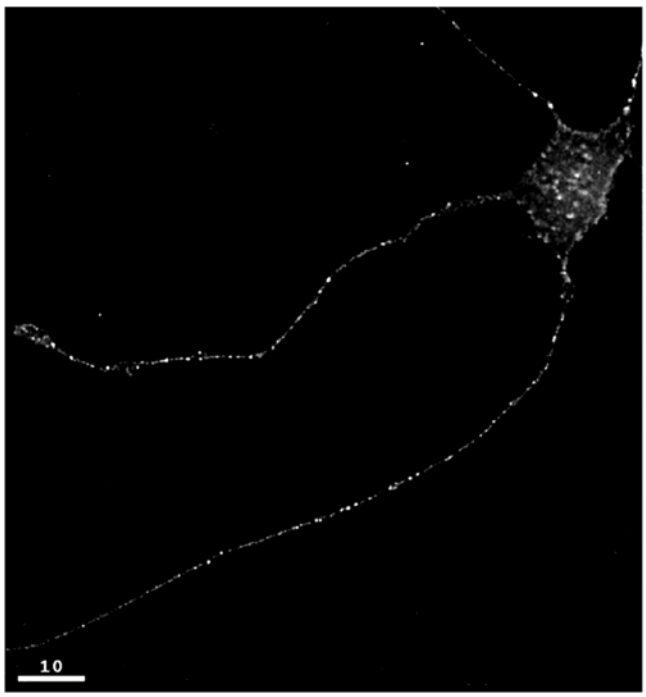

Fig. 2. Deblurred image of a living PC12 cell expressing NCS-1-EYFP. All aspects of distribution that are visible in this image were also visible in images that were not deblurred. Bar, 10 μm.

The distributions of NCS-1-EYFP and NCS-1 in differentiated PC12 cells were assayed using fluorescence microscopy. Fig. 2 shows a deblurred image of the distribution of NCS-1-EYFP in a living, differentiated PC12 cell. NCS-1-EYFP in part exhibits a punctate distribution, strongly suggesting that some NCS-1-EYFP is present on vesicles or other organelles. NCS-1-EYFP also, in part, exhibits a diffuse distribution, strongly suggesting that some NCS-1-EYFP is also present in the cytosol. This diffuse component is unlikely to arise simply from out-of-focus light because hybrid proteins that are packaged exclusively in constitutively secreted vesicles or SGs do not produce a diffuse background in deblurred images (Lochner et al., 1998). Finally, NCS-1-EYFP is distributed throughout the cell body, neurites and growth cones. The distributions of endogenous NCS-1 and overexpressed NCS-1 in wild-type and stably transfected cells were similar (data not shown).

Fluorescence microscopy was also used to show that NCS-1-EYFP colocalizes partially with markers for SLMVs but not with markers for SGs in differentiated PC12 cells. Fig. 3 shows representative high-magnification images of termini and growth cones of PC12 cells expressing NCS-1-EYFP that were

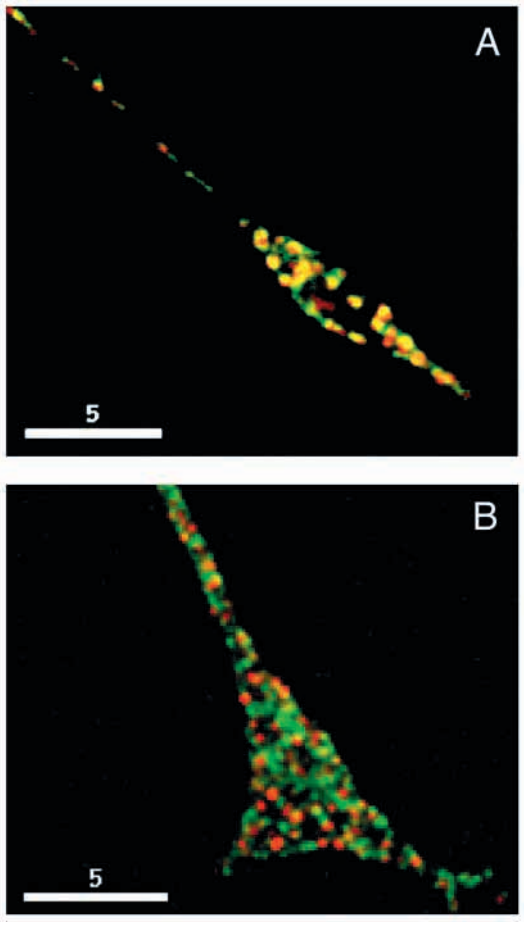

Fig. 3. Representative dual-color images that demonstrate (A) extensive colocalization of NCS-1-EYFP and endogenous synaptophysin and (B) minor colocalization of NCS-1-EYFP and endogenous SgII. NCS-1-EYFP is shown in green, and synaptophysin and SgII are shown in red. Areas of overlap appear yellow. Bars, 5 μm.

immunostained for endogenous synaptophysin or SgII. Significantly, regions devoid of NCS-1-EYFP are also devoid of synaptophysin. Moreover, in Fig. 3A, 73% of the puncta containing NCS-1-EYFP overlap with puncta containing synaptophysin. Overall, 165 puncta containing NCS-1-EYFP were counted in three representative double-labeled cells, and the overlap was 75±7%(±s.d.). By contrast, overlap with SgII (Fig. 3B) and endosomal markers (data not shown) is minor. The absence of NCS-1 from SGs was also demonstrated using immunoelectron microscopy (see below).

The data presented above show that NCS-1-EYFP and synaptophysin colocalize partially in differentiated PC12 cells. Moreover, NCS-1 and synaptophysin colocalize partially in undifferentiated PC12 cells (McFerran et al., 1998). Partial colocalization with synaptophysin suggests, but does not prove, that NCS-1 is associated with SLMVs because synaptophysin is present on a spectrum of organelles, including endosomes, transport vesicles and SLMVs (Clift-O'Grady et al., 1990; Linstedt and Kelly, 1991; Regnier-Vigouroux et al., 1991; de Wit et al., 1999). Thus, further experiments are required to demonstrate conclusively that NCS-1 binds to SLMVs. To this end, we conducted TIRFM experiments.

TIRFM was used to show that NCS-1-EYFP is present in growth cones on organelles that undergo regulated exocytosis. Fig. 4A shows a TIRFM image of a growth cone of a PC12 cell expressing NCS-1-EYFP. The image shows diffuse and punctate fluorescence, consistent with the presence of NCS-1-EYFP on the plasma membrane and on membrane-apposed organelles (i.e. organelles within the ~70 nm evanescent field depth).

Fig. 4B shows images of an NCS-1-EYFP-labeled vesicle that fused with the plasma membrane after electrical stimulation. Two features of the images indicate that this vesicle underwent fusion. First, the vesicle brightened (see also Fig. 4C), indicating that the vesicle moved toward the membrane into a brighter evanescent field and/or flattened onto the plane of the membrane after electrical stimulation. Second, the vesicle fluorescence spread, indicating that the vesicle fused with the membrane.

Fig. 4C shows these trends in a quantitative form as plots of the temporal dependence of the average fluorescence signal originating in circles and circular annuli surrounding membrane-apposed puncta before and after electrical stimulation. For the three different vesicles analyzed here, the fluorescence increased and then decreased in circles and annuli after stimulation, again implying an increase in fluorophore proximity to the membrane followed by fluorophore spreading away from the fusion site in the plane of the membrane over distances of the order of the size of the annulus and for time scales of the order of ~200 milliseconds (Zenisek et al., 2000). Over longer time scales, NCS-1-EYFP may move away from the membrane if it undergoes endocytosis and/or dissociates from the membrane.

Fig. 4D shows an average of 10 curves obtained from 10 different vesicles that underwent stimulation-dependent exocytosis, including those shown in Fig. 4C, normalized to maximum brightness and aligned to time of fusion. This average trace shows that the peak intensity in annuli lags behind the peak intensity in circles.

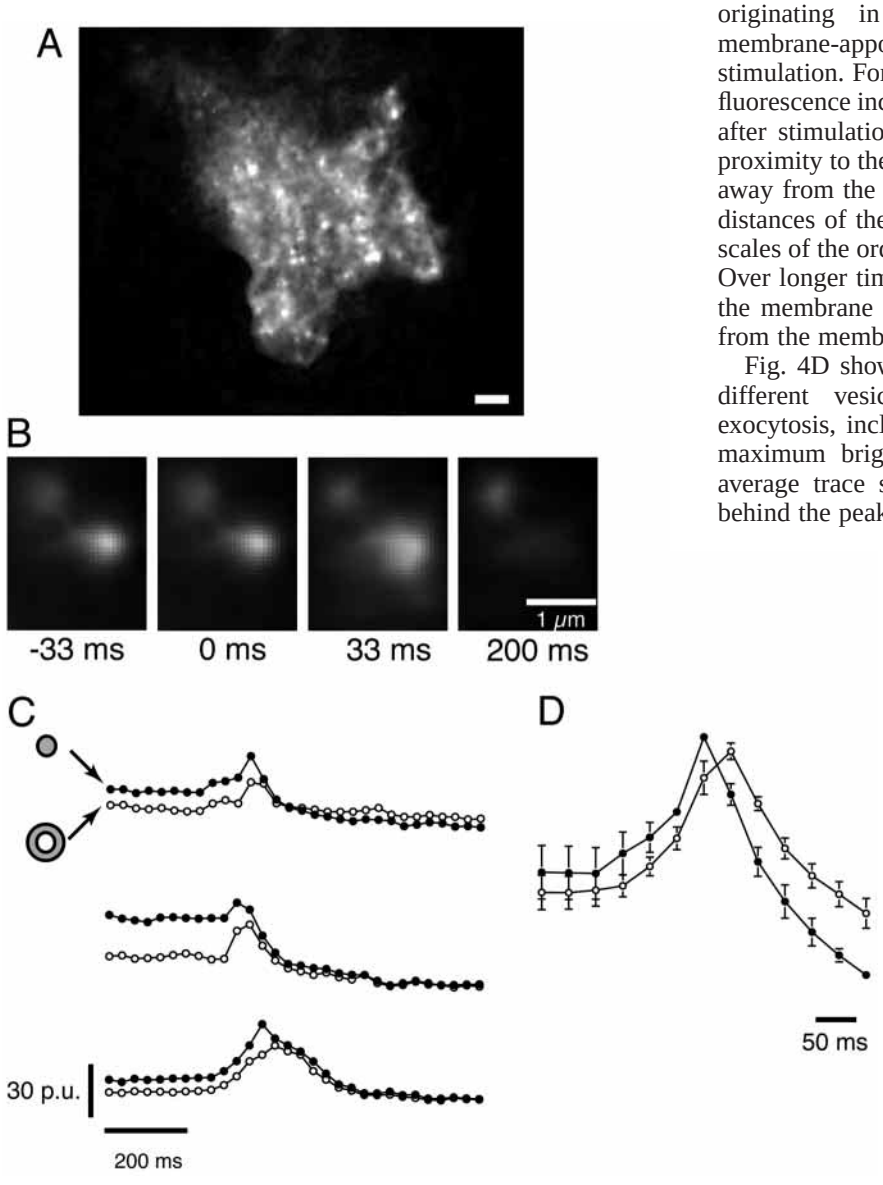

Fig. 4. TIRFM image of a growth cone (A) showing the distribution of NCS-1-EYFP on plasma-membrane-apposed puncta before electrical stimulation. Bar, 2 μm. (B) Images showing the changes in the appearance of a vesicle that underwent stimulation-dependent exocytosis. 33 milliseconds after application of the stimulus, the vesicle fluorescence was widened relative to its initial fluorescence, and 200 milliseconds after application of the stimulus, the vesicle essentially was invisible as its associated fluorescence had spread into the background. Bar, 1 μm. Individual (C) and averaged (D) curves showing fluorophore movement toward the plasma membrane and spreading of fluorescence after electrical stimulation. Data obtained from circles and annuli are represented by closed and open circles, respectively. Fluorescence is expressed in pixel units (P.U.). Bars, 200 milliseconds and 50 milliseconds.

To compute the percentage of plasma-membrane-apposed NCS-1-EYFP-labeled vesicles that undergo stimulation-dependent exocytosis from growth cones of PC12 cells, we quantified the number of puncta per square micron that were excited by the evanescent field and the number that exhibited the post-stimulation behaviors shown in Fig. 4C,D. The average density was 1.04±0.2 μm^{-2} (n=24 cells). After application of a single current pulse, which induces an action potential (Brandt et al., 1976) and a long lasting Ca^{2+} transient in chromaffin cells, the average percentage of puncta that spread and disappeared within ~10 seconds (calculated by computing percentages from different growth cones and averaging the results) was 71±12% (n=16 cells; 793 vesicles). Thus, a substantial fraction of plasma-membrane-apposed vesicles labeled with NCS-1-EYFP undergo stimulation-dependent exocytosis.

For comparative purposes, we also conducted TIRFM experiments on cells expressing VAMP-EGFP, a hybrid consisting of vesicle-associated membrane protein fused to EGFP, and obtained similar results. Thus, TIRFM strongly suggests that some NCS-1-EYFP-bearing puncta, like VAMP-EGFP-bearing puncta, fuse with the plasma membrane following stimulation. The NCS-1-EYFP-bearing organelles that undergo stimulation-dependent exocytosis most probably are SLMVs (see Discussion).

Taken together, our fractionation and microscopy data indicate that NCS-1 and NCS-1-EYFP are distributed similarly in PC12 cells and that both proteins are present in large part on organelles containing synaptophysin. Moreover, our data show that NCS-1-EYFP is present in growth cones, in part, on SLMVs.

Properties of organelles that bind to NCS-1

The morphological properties of organelles that bind to NCS-1 were studied further using fluorescence and electron microscopy.

Fluorescence microscopy was used to characterize the apparent average morphology of organelles that bind to NCS-1-EYFP, without distinguishing different types of organelles. In fluorescence images, organelles that bind to NCS-1-EYFP generally are vesicular. However, some organelles are elongate 'tubulovesicles'. Fig. 5A-D shows time-lapse images of a tubulovesicular organelle transporting NCS-1-EYFP along a neurite. The length of this organelle varied during observation, reaching a maximum of 1.3 μm in Fig. 5D as the organelle moved down the neurite at a speed of ~0.4 μm/second. Of this 1.3 μm, less than ~0.24 μm (~0.4 μm/seconds×0.6 seconds) reflects movement during the 0.6 second exposures times, implying that the true maximum length was at least ~1.0 μm. The width was ~0.4 μm. Organelles containing the hybrid proteins synaptophysin-EGFP and VAMP-EGFP are also predominantly vesicular (data not shown).

Immunoelectron microscopy was used to study organelle morphology and NCS-1-EYFP distribution at high resolution. Fig. 6 shows micrographs of undifferentiated PC12 cells expressing NCS-1-EYFP. Although NCS-1-EYFP was expressed variably, in all cells examined a consistent amount of NCS-1 immunoreactivity was detected on the membrane of vesicles and tubulovesicular organelles, some of which were just below the plasma membrane (Fig. 6B-D, Table 1). On the other hand, no significant NCS-1 immunoreactivity was detected on the membrane of SGs (Fig. 6A,D, Table 1) or on mitochondria and nuclei (Fig. 6, Table 1). In addition, no

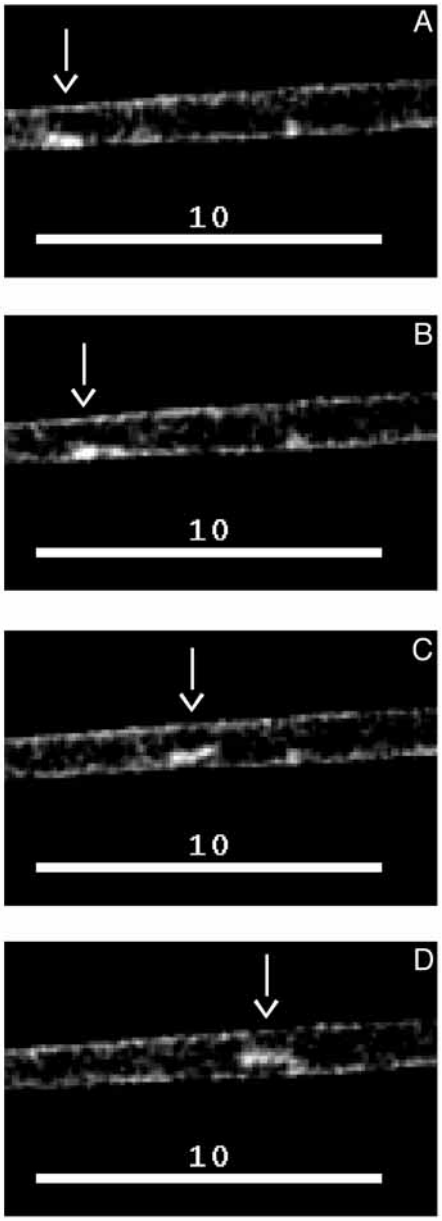

Fig. 5. Time-lapse images showing a tubulovesicular organelle containing NCS-1-EYFP (arrows). Bars, 10 μm.

Table 1. Quantification of NCS-1-EYFP labeling in PC12 cells

Organelle	Vesicular elements	Mitochondria	SGs	Nuclei
Gold particles/μm^2	439±170	18±14	3±2	2±1

Data were obtained from at least two separate experiments. Values are the mean ±s.d. Vesicular elements labeled for NCS-1-EYFP represent 11±6% of the total tubulovesicular elements identified in the micrographs. The density of gold particles over corresponding control sections ranged from 3-12 particles/μm^2.

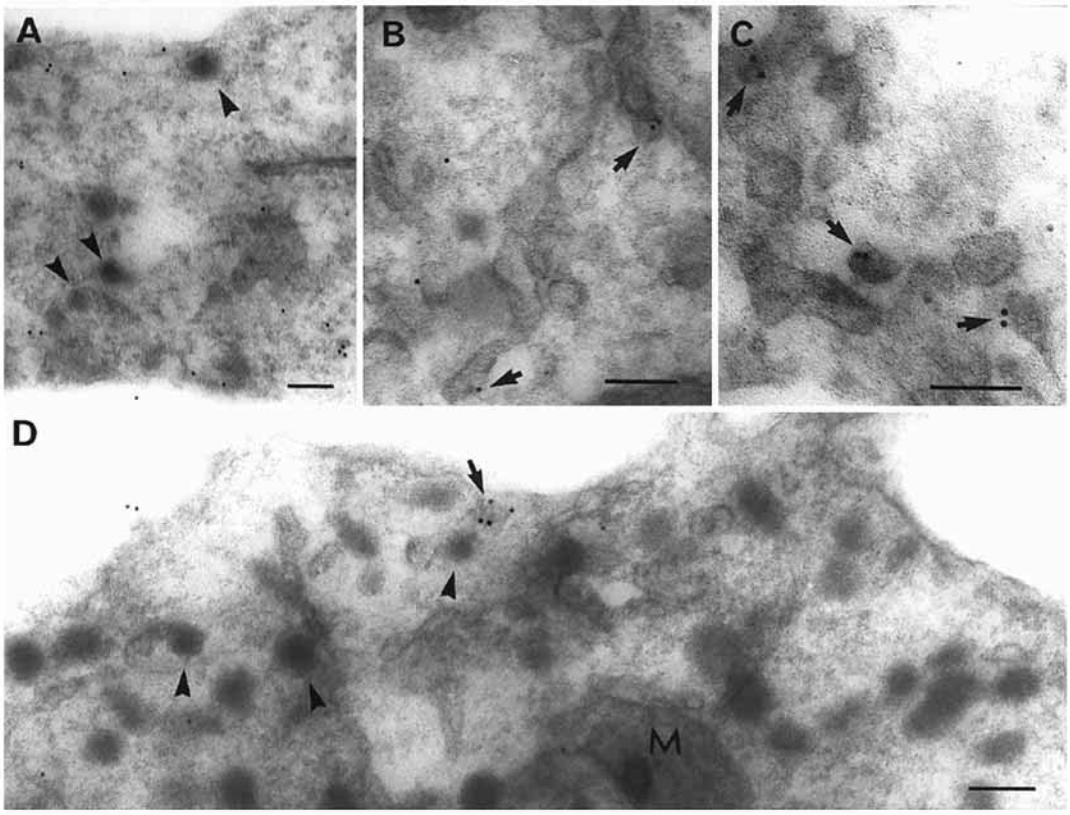

Fig. 6. Immunoelectron micrographs showing the morphology of organelles containing NCS-1 at high resolution in PC12 cells. Most immunoreactivity is likely to arise from NCS-1-EYFP because endogenous NCS-1 is much less abundant than NCS-1-EYFP. Immunoreactivity is partially associated with clear vesicles and tubulovesicular organelles (arrows in B-D) but is absent from SGs (arrowheads in A and D). M, mitochondrion. Bars, 100 nm.

significant immunoreactivity was observed when the primary antibody was substituted with rabbit IgG or was omitted.

Dynamics of organelles labeled by NCS-1 and synaptophysin

The dynamics of organelles labeled by NCS-1 and synaptophysin were studied using wide-field fluorescence microscopy and TIRFM.

Fig. 7A shows a dual-color image of the time-dependent distribution of vesicles that bind to NCS-1-EYFP in a living, differentiated PC12 cell. For comparative purposes, Fig. 7B shows a similar image of the distribution of vesicles containing synaptophysin-EGFP. Associated movies can be viewed at http://www.lclark.edu/~bethe/SLMV/ or jcs.biologists.org/supplemental. Here, green shows vesicles initially, red shows vesicles 20 seconds later and yellow shows overlap of green and red. Most overlap is lost within 20 seconds, showing that most vesicles move substantially over a time scale of <20 seconds. This is true even for growth cones, demonstrating that many vesicles containing SLMV proteins in growth cones are mobile.

Significantly, there is some yellow remaining after 20 seconds, corresponding to vesicles located along neurites or near the periphery of their growth cones. This suggests that some vesicles have docked at these sites. There is also some yellow near the somatic cell surface, where vesicles tend to accumulate.

In the case of wide-field microscopy, we tracked ~70 vesicles in five representative PC12 cells. We tracked many organelles, each for as long as possible, to minimize trajectory bias. Fig. 8A shows 14 trajectories generated by vesicles in the cell in Fig. 7A, all superimposed on an outline of the cell. These trajectories were selected for display because they illustrate the spectrum of dynamic behaviors exhibited by vesicles transporting NCS-1-EYFP.

Vesicles *a-e* in Fig. 8A provide examples of rapid, substantially directed vesicle motion. Rapid, directed motion occurs in cell bodies (vesicles *a-d*) and in neurites (vesicle *e*). Such motion is directed both toward and away from the plasma membrane in cell bodies and both anterograde and retrograde in neurites.

Vesicles *f-h* in Fig. 8A provide examples of random motion. Random motion primarily was observed in the cell body and in growth cones. In some cases, random motion appears to be truly diffusive, as demonstrated in Fig. 9.

Vesicles *i-n* in Fig. 8A provide examples of no motion. Immobility primarily was observed along neurites of differentiated PC12 cells and near the periphery of growth cones.

In the case of TIRFM, we tracked ~50 vesicles in five representative growth cones. Fig. 8B shows three trajectories generated by vesicles in the growth cone in Fig. 4A superimposed on an outline of the growth cone. In this case, the vesicles were SLMVs because ~5 seconds after the trajectories were generated, the cells were stimulated and the vesicles underwent exocytosis. Overall, ~20% of SLMVs were relatively immobile before they underwent exocytosis. Correspondingly, ~80% were mobile before they underwent exocytosis, indicating that they were not docked or permanently tethered to cytoskeletal constituents before exocytosis.

Fig. 9A-D characterizes the dynamics of individual vesicles and SLMVs quantitatively, showing representative plots of $\langle r^2 \rangle^{1/2}$ versus t and $\langle r^2 \rangle$ versus t that were derived from

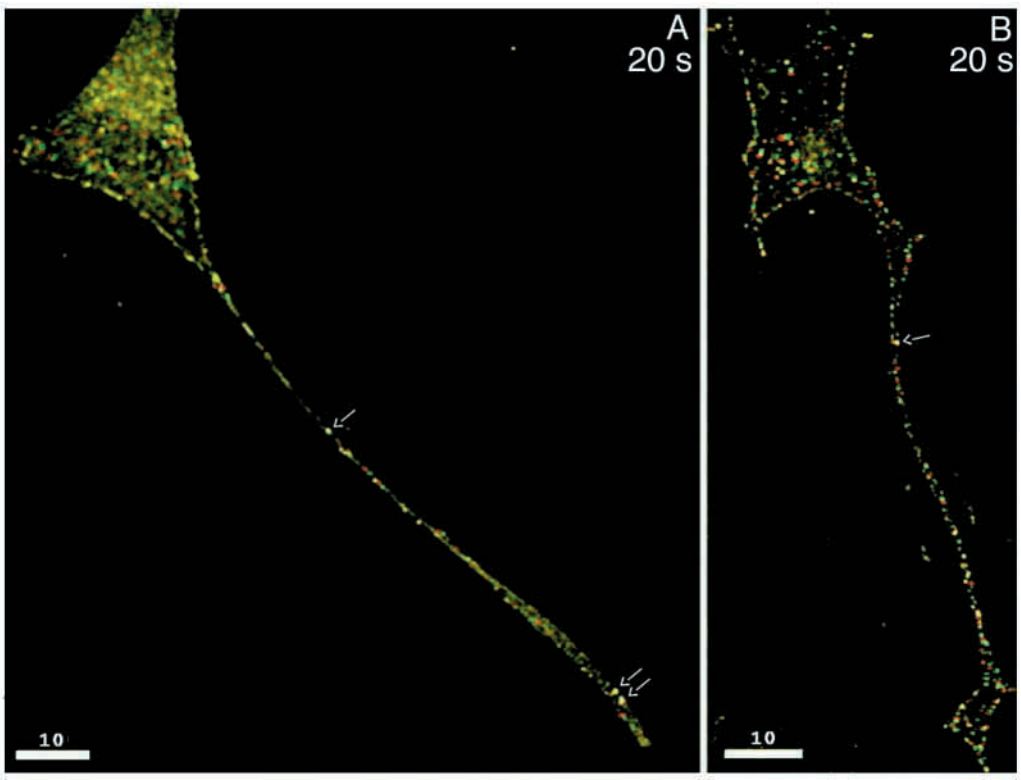

Fig. 7. Dual-color images showing that the distribution of vesicles containing (A) NCS-1-EYFP and (B) synaptophysin-EGFP changes appreciably in 20 seconds. After 20 seconds, overlap (yellow) is associated mostly with vesicles along neurites (arrows) and with cytosolic NCS-1-EYFP, which generates a diffuse yellow background in the cell in A. Bars, 10 μm.

selected vesicle trajectories shown in Fig. 8A and from selected SLMV trajectories (not shown).

Fig. 9A shows that vesicles *a* and *e*, which appear in Fig. 8A to have undergone rapid and directed motion, generated trajectories that could be described quantitatively by the directed motion term v^2t^2 in Equation 1. The speeds v computed from slopes of the $<r^2>^{1/2}$ versus t plots were 0.16 μm/second (*a*) and 0.34 μm/second (*e*). The average v for vesicles undergoing directed motion was 0.25±0.16 μm/second. In contrast, Fig. 9B shows that vesicle *g*, which appears in Fig. 8A to have undergone random motion, generated a trajectory that could be described quantitatively by the diffusive motion term $4Dt$ in Equation 1. Vesicle *g* diffused very slowly; the diffusion coefficient D computed from the slope of the $<r^2>$ versus t plot was 5.4×10^{-11} cm^2/second.

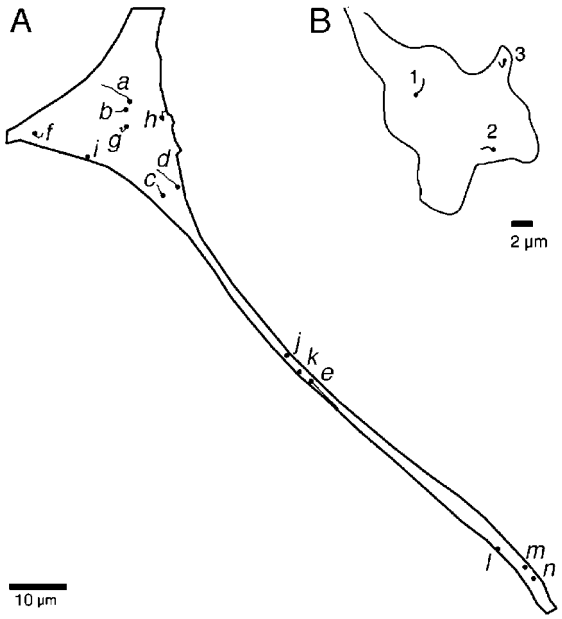

Fig. 8. Trajectories of vesicles in (A) the cell in Fig. 7A and (B) the growth cone in Fig. 4A, superimposed on outlines of the cell and growth cone. Starting vesicle positions are labeled with a closed circle. Not all of these trajectories were generated simultaneously. Bars, 10 μm (A) and 2 μm (B).

Fig. 9C,D shows that SLMVs in growth cones also generated trajectories that could be described quantitatively by either the directed or the diffusive motion term in Equation 1. From plots like these, some SLMVs were found to undergo directed motion, again at speeds of several tenths of a μm/second; others were found to undergo diffusive motion with an average D of 1.68×10^{-9} cm^2/second.

Function of NCS-1 in PC12 cells

The distribution and dynamics data presented above indicate that NCS-1-EYFP is associated with SLMVs in growth cones of PC12 cells. Here, we present complementary functional data that indicate that NCS-1 overexpression enhances SLMV/SG exocytosis under basal conditions and during stimulation by UTP, which activates phosphoinositide-dependent signaling pathways in PC12 cells (Koizumi et al., 1995). To study NCS-1 function, we incubated living PC12 cells with an antibody directed against the luminal domain of synaptotagmin I. This antibody is internalized into RSOs following exocytosis (Marxen et al., 1997; Coco et al., 1998).

Fig. 10A,B shows representative images revealing the

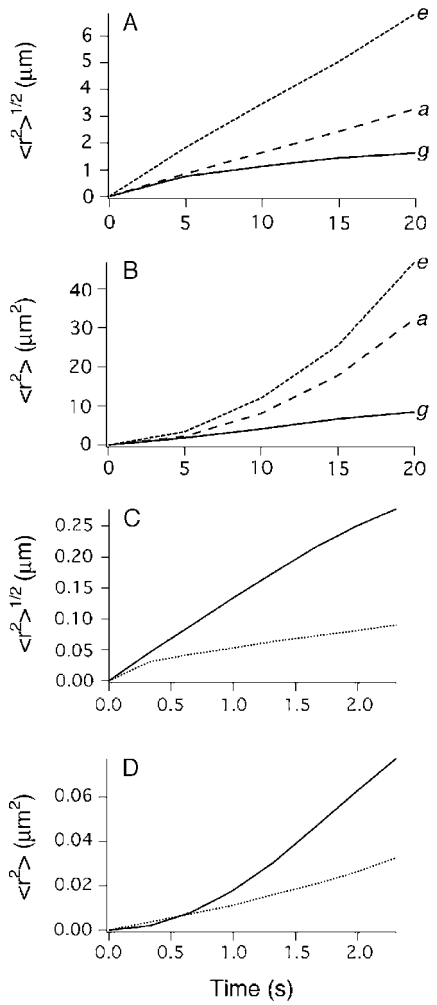

Fig. 9. Plots of (A and C) $\langle r^2\rangle^{1/2}$ versus *t* and (B and D) $\langle r^2\rangle$ versus *t* deduced in part from the trajectories in Fig. 8A. Letters next to the plots identify the trajectories from which the plots were derived. Some values were rescaled so that all plots could be displayed together conveniently. In A, values of $\langle r^2\rangle^{1/2}$ were multiplied by 2.5 for vesicle *g*. In B, values of $\langle r^2\rangle$ were multiplied by three and 20 for vesicles *a* and *g*, respectively. In C and D, values for the dashed curves were multiplied by 2.5 and 25, respectively.

degree of basal internalization of the anti-synaptotagmin I antibody by PC12 cells that contain a control vector and by PC12 cells that overexpress NCS-1 approximately six-fold. Table 2 shows complementary numerical data, which were obtained by quantifying fluorescence signals from ~30 individual cells (for each cell type) using NIH image software. The degree of enhancement in uptake was computed from these data using the ratio $(F_2-F_1)/F_1$, where F_2 and F_1 are the fluorescence signals for overexpressing and control cells, respectively. On average, basal antibody internalization was enhanced ~8% after 15 minutes and ~43% after 45 minutes in the overexpressing cells. By contrast, total synaptotagmin I levels in control and overexpressing cells did not differ, as determined by labeling all synaptotagmin I molecules in fixed cells using an antibody that binds to the cytoplasmic domain of synaptotagmin I (Coco et al., 1998). Specifically, fluorescence signals reflecting total synaptotagmin I content in overexpressing and control cells were 119.8±7.3 (*n*=33) and 122.8±7.1 (*n*=36), respectively.

Fig. 10C,D and Table 2 show representative images and quantitative data revealing the degree of UTP-induced internalization of anti-synaptotagmin I antibody. The degree of enhancement in uptake was computed from the ratio above, where 2 and 1 refer to with UTP and without UTP, respectively. Incubation with 10 μM or 100 μM UTP enhanced internalization by ~40% and ~58%, respectively, for control cells and by ~67% and ~96% for overexpressing cells. The substantially enhanced internalization exhibited by overexpressing UTP-stimulated cells correlated with an increase in the number of puncta near the cell periphery (Fig. 10D).

Discussion

Distribution, dynamics and interaction of NCS-1 with RSOs

The distribution, dynamics and interaction of NCS-1 with RSOs are not completely understood. Here we have studied NCS-1 with a spectrum of biochemical and biophysical techniques and thereby resolved many of the uncertainties surrounding these attributes of NCS-1. For example, we have determined that NCS-1 localizes to clear organelles, the cytosol and neurites and their growth cones in PC12 cells.

We have also determined the mechanism underlying transport of NCS-1 in differentiated PC12 cells. Specifically, we have shown that organelle-based, fast axonal transport conveys some NCS-1 to the growth cone. Fast axonal transport of NCS-1 is bidirectional along neurites and occurs predominantly on vesicular organelles. Vesicular organelles also transport synaptophysin and VAMP along neurites of PC12 cells, and NCS-1, in part, is co-transported with synaptophysin.

Table 2. Quantification of uptake of anti-synaptotagmin antibody in PC12 cells

	Cells containing vector control (normalized to 15 minutes basal recycling of vector control cells)	Cells overexpressing NCS-1 (normalized to 15 minutes basal recycling of vector control cells)	Cells overexpressing NCS-1 (normalized to 15 minutes basal recycling of overexpressing cells)
Basal (buffered saline for 15 minutes)	100.0±3.7 (*n*=35)	107.9±3.8 (*n*=38)	100.0±3.6
Basal (buffered saline for 45 minutes)	111.8±3.3 (*n*=39)	160.4±3.9 (*n*=34)	148.6±3.6
UTP (10 μM for 15 minutes)	139.6±14.1 (*n*=33)	180.6±5.9 (*n*=32)	167.3±5.5
UTP (100 μM for 15 minutes)	157.9±12.2 (*n*=29)	211.5±8.8 (*n*=35)	196.0±8.2

Uptake is expressed as a percentage relative to cells containing the vector control in buffered saline for 15 minutes (data columns 1 and 2) or as a percentage relative to cells overexpressing NCS-1 in buffered saline for 15 minutes (data column 3). Data were obtained from cells from three different cover slips for each cell type.

Finally, we have determined that NCS-1 interacts with RSOs. Specifically, we have found that electrical stimulation induces fusion of NCS-1-EYFP-bearing puncta with the plasma membrane of growth cones, strongly suggesting that NCS-1-EYFP is present on RSOs in growth cones. These RSOs could be either SLMVs or SGs. However, we have found that NCS-1-EYFP does not localize with SGs in electron micrographs and that NCS-1-EYFP colocalizes with markers for SLMVs but not with markers for SGs in western blots and fluorescence micrographs. These localization results strongly suggest that NCS-1 is associated preferentially with SLMVs in growth cones of differentiated PC12 cells, providing support for a function in neurotransmission.

Our observations about NCS-1 distribution have several additional implications. First, they show that NCS-1 is distributed appropriately to interact with putative targets, such as PtdIns 4-kinase beta, that are associated with neurotransmitter-containing vesicles and plasma membranes of mammalian neuroendocrine cells and neurons (Wiedemann et al., 1998) (E.T., unpublished). Second, they support the hypothesis that myristoylated NCS-1 stimulates the activity of PtdIns 4-kinase beta while these proteins are bound to a membranous compartment (Zhao et al., 2001), such as the surface of an SLMV or the plasma membrane.

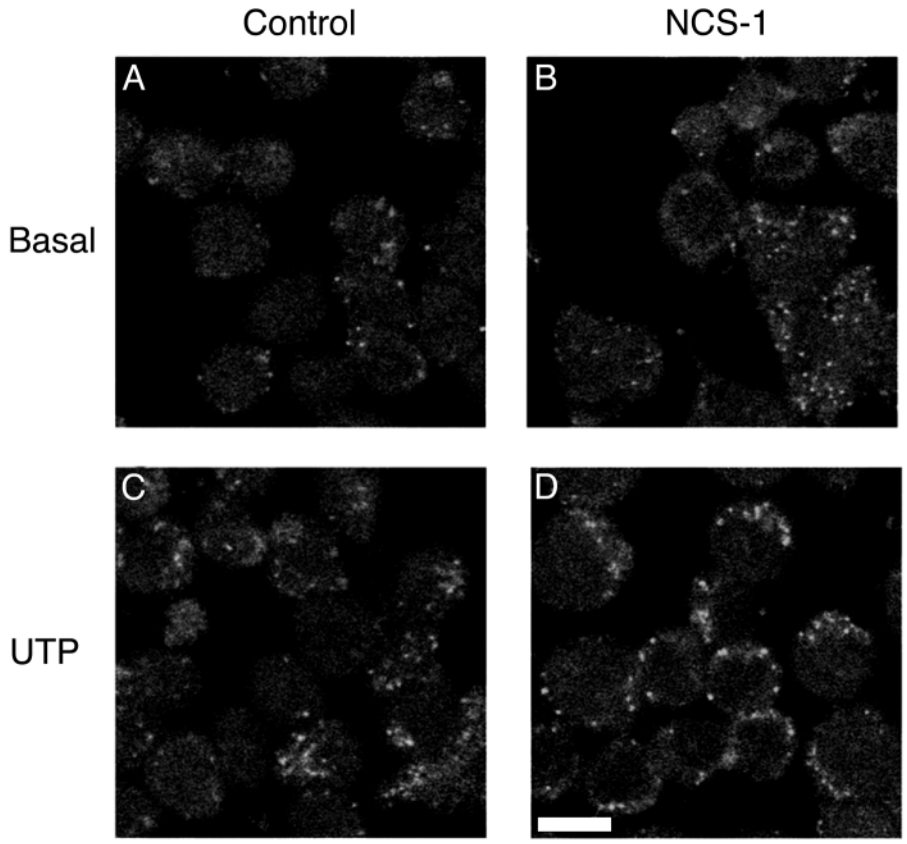

Fig. 10. Confocal images showing the uptake of anti-synaptotagmin antibody by PC12 cells that contain a vector control (Control) and PC12 cells that overexpress NCS-1 (NCS-1) under basal and UTP-stimulation (UTP) conditions. Images correspond to 45 minutes of basal uptake (A,B) and 15 minutes of UTP-stimulated uptake (C,D). Bar, 20 μm.

Function of NCS-1

The function of NCS-1 is also incompletely understood. Several studies suggest a role in regulated exocytosis and phosphoinositide signaling, but the precise function of NCS-1 remains unknown (Pongs et al., 1993; Olafsson et al., 1995; McFerran et al., 1998; McFerran et al., 1999; Hendricks et al., 1999).

Here we have demonstrated that NCS-1 overexpression enhances basal and UTP-stimulated exocytosis of RSOs in PC12 cells. NCS-1's role in basal exocytosis is not well understood, in part because pertinent past studies have produced inconsistent results (Rivosecchi et al., 1994; Olafsson et al., 1995; McFerran et al., 1998; Chen et al., 2001). Consistent with results obtained previously by acute infusion of frequenin in *Xenopus* (Olaffson et al., 1995), our overexpression data implicate NCS-1/frequenin in the enhancement of basal exocytosis and extend this function to mammalian cells. As discussed below, this enhancement could reflect a role for NCS-1 in the production of phosphatidylinositol 4,5-bisphosphate (PtdIns(4,5)P_2) and the involvement of PtdIns(4,5)P_2 in regulating many aspects of membrane trafficking (Jost et al., 1998; Martin, 2001).

NCS-1's role in stimulated exocytosis is better understood, in part because NCS-1 and frequenin have been shown to enhance electrically stimulated exocytosis in several organisms and cell types (Pongs et al., 1993; Rivosecchi et al., 1994; Olafsson et al., 1995; Chen et al., 2001). Here we have extended these results to include UTP-stimulated exocytosis of RSOs in PC12 cells. UTP-stimulated exocytosis is distinct from previously studied exocytotic processes, because it is mediated by Ca^{2+} release from intracellular stores; moreover, this release is initiated when PtdIns(4,5)P_2 serves as a substrate for phospholipase C (PLC) after UTP binds to G-protein-coupled receptors on PC12 cells (Koizumi et al., 1995).

We were interested in studying NCS-1's role in UTP-stimulated exocytosis because current data suggest that NCS-1 activates PtdIns 4-kinase beta, an enzyme involved in the synthesis of PtdIns(4,5)P_2 (Hendricks et al., 1999; Martin, 2001). In light of this, NCS-1 overexpression might enhance UTP-stimulated exocytosis, as observed here, by enhancing local levels of PtdIns(4,5)P_2 and providing additional substrate for PLC. Indeed, NCS-1 overexpression does enhance levels of PtdIns(4,5)P_2 (S.K., unpublished), strengthening this possibility. Moreover, NCS-1 overexpression also enhances ATP-stimulated hormone release from PC12 cells (McFerran et al., 1998), perhaps via a similar mechanism.

On the basis of our microscopy and biochemical data, it is tempting to speculate that NCS-1 enhances RSO exocytosis

primarily by enhancing SLMV exocytosis. In agreement with this, NCS-1 recently has been shown to increase release from SVs in a neuroblastoma-myocyte co-culture model (Chen et al., 2001).

Dynamics of SLMVs in growth cones

Here we summarize the attributes of SLMV dynamics as revealed in our TIRFM studies and analyze their potential implications.

TIRFM demonstrates the existence of both mobile and immobile pools of SLMVs in growth cones of unstimulated PC12 cells. The dynamics of some of the mobile SLMVs is best described as diffusive with an average diffusion coefficient D of 1.68×10^{-9} cm^2/second. Despite this mobility, the motion of these SLMVs is hindered substantially. To demonstrate this, we compare the measured average diffusion coefficient with the calculated diffusion coefficient of an equivalently sized spherical particle in dilute solution using the Stokes-Einstein relationship $D_{\text{dilute}}=k_BT/6\pi\eta r$ (Berg, 1983). Here, k_B is Boltzmann's constant, T is the absolute temperature (~300 K), η is the solution viscosity (~10^{-3} Pa second) and r is the radius of the sphere (~25 nm) (Cutler and Cramer, 1990; de Wit et al., 1999). The calculated diffusion coefficient is 8.8×10^{-8} cm^2/second. Thus, the average D of SLMVs in growth cones is ~$0.02D_{\text{dilute}}$, indicating that diffusion of SLMVs is hindered substantially.

Considerable interest has been directed at delineating the factors that dictate organelle motion in nerve termini and growth cones. In this context, actin has been postulated to play two different roles. Actin may facilitate motion by acting as a track for myosin-based motor proteins (Evans and Bridgman, 1995; Ryan, 1999; Cole et al., 2000). Alternatively, actin may hinder motion, especially near the plasma membrane, where cortical actin may present a barrier to transport and exocytosis (Trifaro and Vitale, 1993; Burke et al., 1997; Abney et al., 1999; Steyer and Almers, 1999). Our data are consistent with actin both facilitating and hindering the motion of SLMVs. In particular, our data suggest that in some cases SLMV motion is facilitated, because they show that some plasma-membrane-apposed SLMVs, which move in an actin-dominated milieu (Evans and Bridgman, 1995), undergo fast, directed motion. Our data also suggest that in some cases motion is hindered, because they show that some plasma-membrane-apposed SLMVs are immobile and that some undergo diffusion at rates that are reduced substantially relative to dilute solution. Immobility or hindrance of SLMV motion by actin could arise from long-lived/transient organelle binding, steric effects or both (Kao et al., 1993).

Comparison of the dynamics of SLMVs and SGs in growth cones

Wide-field fluorescence microscopy and TIRFM have been used in conjunction with GFP hybrids to study the dynamics of SGs in growth cones of PC12 cells (Burke et al., 1997; Abney et al., 1999; Han et al., 1999). Here we compare the dynamics of SGs and SLMVs in growth cones, highlighting similarities and differences.

Recent data suggest that SGs generally are mobile in growth cones of unstimulated PC12 cells and that SGs undergo both diffusive and directed motion. Diffusive motion occurs primarily in central and peripheral parts of growth cones, where most SGs diffuse two to four orders of magnitude more slowly than similarly sized spheres in dilute solution (Abney et al., 1999; Han et al., 1999). Directed motion occurs primarily in proximal parts of growth cones, where a subset of SGs undergoes rapid, directed motion at fast axonal transport speeds (Abney et al., 1999).

Here we have shown that SLMVs generally are also mobile in growth cones of unstimulated PC12 cells and that SLMVs also undergo both diffusive and directed motion. Interestingly, however, the diffusion of SLMVs in growth cones is less hindered than the diffusion of SGs. One possible origin for this difference is that the growth cone is a highly congested environment, containing a high density of organelles as well as microtubules and actin filaments (Forscher and Smith, 1988; Hirokawa et al., 1989). Such congestion is known to hinder the motion of larger structures, such as SGs, more significantly than the motion of smaller structures, such as SLMVs (Luby-Phelps et al., 1987). Thus, congestion (and/or binding differences) may give rise to the observed differences in SG and SLMV mobility in growth cones.

Comparison of transport in differentiated neuroendocrine cells and neurons

In this work, we studied the organelles that transport NCS-1, synaptophysin and VAMP within differentiated neuroendocrine cells. Here we compare our results with analogous results obtained from studies of transport in dorsal root ganglion (DRG) and hippocampal neurons.

Comparison of transport organelles in differentiated neuroendocrine cells and neurons reveals considerable diversity in organelle morphology and transport properties. For example, organelles transporting synaptophysin in differentiated PC12 cells are similar in morphology and transport properties to their analogs in hippocampal neurons; in both cell types, the organelles are vesicular, with some undergoing rapid, nonrandom motion and others undergoing random motion or no motion (Kaether et al., 2000). By contrast, organelles transporting synaptophysin in differentiated PC12 cells differ in morphology from their analogs in DRG neurons, and organelles transporting VAMP differ similarly from their analogs in hippocampal neurons. In these latter cases, the organelles in neurons are more tubular (Nakata et al., 1998; Ahmari et al., 2000). Clearly, the morphology of carrier organelles for these proteins depends on both the cell type and the protein.

We thank James Abney and Daniel Axelrod for their comments on the manuscript. This work was supported by NSF (#BIR-9510226), NIH (#GM61539) and Research Corporation (#CC3819) grants (to B.A.S.), and by the CNR-Target Project on Biotechnology and EU program TMR ERBB104CT960058 (to P.R.). J.R. and A.J. were supported by the NSERC and MRC of Canada.

References

Abney, J. R., Meliza, C. D., Cutler, B., Kingma, M., Lochner, J. E. and Scalettar, B. A. (1999). Real-time imaging of the dynamics of secretory granules in growth cones. *Biophys. J.* **77**, 2887-2895.

Ahmari, S. E., Buchanan, J. and Smith, S. J. (2000). Assembly of

presynaptic active zones from cytoplasmic transport packets. *Nat. Neurosci.* **3**, 445-451.

Axelrod, D. (1989). Total internal reflection fluorescence microscopy. *Methods Cell Biol.* **30**, 245-270.

Bennett, M. K. (1997). Ca^{2+} and the regulation of neurotransmitter secretion. *Curr. Opin. Neurobiol.* **7**, 316-322.

Berg, H. (1983). *Random Walks in Biology.* Princeton, NJ: Princeton University Press.

Brandt, B. L., Hagiwara, S., Kidokoro, Y. and Miyazaki, S. (1976). Action potentials in the rat chromaffin cell and effects of acetylcholine. *J. Physiol.* (London) **263**, 417-439.

Burgess, T. L. and Kelly, R. B. (1987). Constitutive and regulated secretion of proteins. *Annu. Rev. Cell Biol.* **3**, 243-293.

Burgoyne, R. D. and Weiss, J. L. (2001). The neuronal calcium sensor family of Ca^{2+}-binding proteins. *Biochem. J.* **353**, 1-12.

Burke, N. V., Han, W., Li, D., Takimoto, K., Watkins, S. C. and Levitan, E. S. (1997). Neuronal peptide release is limited by secretory granule mobility. *Neuron* **19**, 1095-1102.

Calegari, F., Coco, S., Taverna, E., Bassetti, M., Verderio, C., Corradi, N., Matteoli, M. and Rosa, P. (1999). A regulated secretory pathway in cultured hippocampal astrocytes. *J. Biol. Chem.* **274**, 22539-22547.

Chen, X., Zhong, Z., Yokoyama, S., Bark, C., Meister, B., Berggren, P., Roder, J., Higashida, H. and Jeromin, A. (2001). Overexpression of rat neuronal calcium sensor-1 in rodent NG108-15 cells enhances synapse formation and transmission. *J. Physiol.* **532**, 649-659.

Clift-O'Grady, L., Linstedt, A. D., Lowe, A. W., Grote, E. and Kelly, R. B. (1990). Biogenesis of synaptic vesicle-like structures in a pheochromocytoma cell line PC-12. *J. Cell Biol.* **110**, 1693-1703.

Coco, S., Verderio, C., de Camilli, P. and Matteoli, M. (1998). Calcium dependence of synaptic vesicle recycling before and after synaptogenesis. *J. Neurochem.* **71**, 1987-1992.

Cole, J. C., Villa, B. R. S. and Wilkinson, R. S. (2000). Disruption of actin impedes transmitter release in snake motor nerve terminals. *J. Physiol.* **525**, 579-586.

Cutler, D. F. and Cramer, L. P. (1990). Sorting during transport to the surface of PC12 cells: divergence of synaptic vesicle and secretory granule proteins. *J. Cell Biol.* **110**, 721-730.

De Camilli, P. and Jahn, R. (1990). Pathways to regulated exocytosis in neurons. *Annu. Rev. Physiol.* **52**, 625-645.

de Wit, H., Lichtenstein, Y., Geuze, H. J., Kelly, R. B., van der Sluijs, P. and Klumperman, J. (1999). Synaptic vesicles form by budding from tubular extensions of sorting endosomes in PC12 cells. *Mol. Biol. Cell* **10**, 4163-4176.

Evans, L. L. and Bridgman, P. C. (1995). Particles move along actin filament bundles in nerve growth cones. *Proc. Natl. Acad. Sci. USA* **92**, 10954-10958.

Forscher, P. and Smith, S. J. (1988). Actions of cytochalasins on the organization of actin filaments and microtubules in a neuronal growth cone. *J. Cell Biol.* **107**, 1505-1516.

Halban, P. A. and Irminger, J.-C. (1994). Sorting and processing of secretory proteins. *Biochem. J.* **299**, 1-18.

Han, W., Ng, Y. K., Axelrod, D. and Levitan, E. S. (1999). Neuropeptide release by efficient recruitment of diffusing cytoplasmic secretory vesicles. *Proc. Natl. Acad. Sci. USA* **96**, 14577-14582.

Hendricks, K. B., Wang, B. Q., Schnieders, E. A. and Thorner, J. (1999). Yeast homologue of neuronal frequenin is a regulator of phosphatidylinositol-4-OH kinase. *Nat. Cell Biol.* **1**, 234-241.

Hirokawa, N., Sobue, K., Kanda, K., Harada, A. and Yorifuji, H. (1989). The cytoskeletal architecture of the presynaptic terminal and molecular structure of synapsin 1. *J. Cell Biol.* **108**, 111-126.

Huttner, W. B., Ohashi, M., Kehlenbach, R. H., Barr, F. A., Bauerfeind, R., Braunling, O., Corbeil, D., Hannah, M., Pasolli, H. A., Schmidt, A. et al. (1995). Biogenesis of neurosecretory vesicles. *Cold. Spring Harb. Symp. Quant. Biol.* **60**, 315-327.

Jost, M., Simpson, F., Kavran, J. M., Lemmon, M. A. and Schmid, S. L. (1998). Phosphatidylinositol-4,5-bisphosphate is required for endocytic coat formation. *Curr. Biol.* **8**, 1399-1402.

Kaether, C., Skehel, P. and Dotti, C. G. (2000). Axonal membrane proteins are transported in distinct carriers: a two-color video microscopy study in hippocampal neurons. *Mol. Biol. Cell* **11**, 1213-1224.

Kao, H. P., Abney, J. R. and Verkman, A. S. (1993). Determinants of the translational mobility of a small solute in cell cytoplasm. *J. Cell Biol.* **120**, 175-184.

Koizumi, S., Nakazawa, K. and Inoue, K. (1995). Inhibition by Zn^{2+} of uridine 5′-triphosphate-induced Ca^{2+}-influx but not Ca^{2+}-mobilization in rat phaeochromocytoma cells. *Br. J. Pharmacol.* **115**, 1502-1508.

Linstedt, A. D. and Kelly, R. B. (1991). Synaptophysin is sorted from endocytotic markers in neuroendocrine PC12 cells but not transfected fibroblasts. *Neuron* **7**, 309-317.

Lochner, J. E., Kingma, M., Kuhn, S., Meliza, C. D., Cutler, B. and Scalettar, B. A. (1998). Real-time imaging of the axonal transport of granules containing a tissue plasminogen activator/green fluorescent protein hybrid. *Mol. Biol. Cell* **9**, 2463-2476.

Luby-Phelps, K., Castle, P. E., Taylor, D. L. and Lanni, F. (1987). Hindered diffusion of inert tracer particles in the cytoplasm of mouse 3T3 cells. *Proc. Natl. Acad. Sci. USA* **84**, 4910-4913.

Manivannan, S. and Terakawa, S. (1994). Rapid sprouting of filopodia in nerve terminals of chromaffin cells, PC12 cells, and dorsal root neurons induced by electrical stimulation. *J. Neurosci.* **14**, 5917-5928.

Martin, T. F. J. (1998). Phosphoinositide lipids as signaling molecules: common themes for signal transduction, cytoskeletal regulation, and membrane trafficking. *Annu. Rev. Cell Dev. Biol.* **14**, 231-264.

Martin, T. F. J. (2001). $PI(4,5)P_2$ regulation of surface membrane traffic. *Curr. Opin. Cell Biol.* **13**, 493-499.

Marxen, M., Maienschein, V., Volknandt, W. and Zimmermann, H. (1997). Immunocytochemical localization of synaptic proteins at vesicular organelles in PC12 cells. *Neurochem. Res.* **8**, 941-950.

Matteoli, M., Takei, K., Perin, M. S., Sudhof, T. C. and de Camilli, P. (1992). Exo-endocytotic recycling of synaptic vesicles in developing processes of cultured hippocampal neurons. *J. Cell Biol.* **117**, 849-861.

McFerran, B. W., Graham, M. E. and Burgoyne, R. D. (1998). Neuronal Ca^{2+} sensor 1, the mammalian homologue of frequenin, is expressed in chromaffin and PC12 cells and regulates neurosecretion from dense-core granules. *J. Biol. Chem.* **273**, 22768-22772.

McFerran, B. W., Weiss, J. L. and Burgoyne, R. D. (1999). Neuronal Ca^{2+} sensor 1, characterization of the myristoylated protein, its cellular effects in permeabilized adrenal chromaffin cells, Ca^{2+}-independent membrane association, and interaction with binding proteins, suggesting a role in rapid Ca^{2+} signal transduction. *J. Biol. Chem.* **274**, 30258-30265.

Meyer, T. and York, J. D. (1999). Calcium-myristoyl-switches turn on new lights. *Nat. Cell Biol.* **1**, E93-E95.

Nakamura, T. Y., Pountney, D. J., Ozaita, A., Nandi, S., Ueda, S., Rudy, B. and Coetzee, W. A. (2001). A role for frequenin, a Ca^{2+}-binding protein, as a regulator of Kv4 K^+-currents. *Proc. Natl. Acad. Sci. USA* **98**, 12808-12813.

Nakata, T., Terada, S. and Hirokawa, N. (1998). Visualization of the dynamics of synaptic vesicle and plasma membrane proteins in living axons. *J. Cell Biol.* **140**, 659-674.

Nef, S., Fiumelli, H., de Castro, E., Raes, M. B. and Nef, P. (1995). Identification of neuronal calcium sensor (NCS-1) possibly involved in the regulation of receptor phosphorylation. *J. Recept. Signal Trans. Res.* **15**, 365-378.

Olafsson, P., Wang, T. and Lu, B. (1995). Molecular cloning and functional characterization of the *Xenopus* Ca^{2+}-binding protein frequenin. *Proc. Natl. Acad. Sci. USA* **92**, 8001-8005.

Passafaro, M., Rosa, P., Sala, C., Clementi, F. and Sher, E. (1996). N-type Ca^{2+} channels are present in secretory granules and are transiently translocated to the plasma membrane during regulated exocytosis. *J. Biol. Chem.* **271**, 30096-30104.

Pongs, O., Lindemeier, J., Zhu, X. R., Theil, T., Engelkamp, D., Krah-Jentgens, I., Lambrecht, H. G., Koch, K. W., Schwemer, J., Rivosecchi, R. et al. (1993). Frequenin—a novel calcium-binding protein that modulates synaptic efficacy in the *Drosophila* nervous system. *Neuron* **11**, 15-28.

Regnier-Vigouroux, A., Tooze, S. A. and Huttner, W. B. (1991). Newly synthesized synaptophysin is transported to synaptic-like microvesicles via constitutive secretory vesicles and the plasma membrane. *EMBO. J.* **10**, 3589-3601.

Rivosecchi, R., Pongs, O., Theil, T. and Mallart, A. (1994). Implication of frequenin in the facilitation of transmitter release in *Drosophila*. *J. Physiol.* **474**, 223-232.

Rothman, J. E. (1994). Mechanisms of intracellular protein transport. *Nature* **372**, 55-63.

Rowe, J., Corradi, N., Malosio, M. L., Taverna, E., Halban, P., Meldolesi, J. and Rosa, P. (1999). Blockage of membrane transport and disassembly of the golgi complex by expression of syntaxin 1A in neurosecretion-incompetent cells: prevention by rbSEC1. *J. Cell Sci.* **112**, 1865-1877.

Ryan, T. A. (1999). Inhibitors of myosin light chain kinase block synaptic vesicle pool mobilization during action potential firing. *J. Neurosci.* **19**, 1317-1323.

Saxton, M. J. and Jacobson, K. (1997). Single-particle tracking: applications to membrane dynamics. *Annu. Rev. Biophys. Biomol. Struct.* **26**, 373-399.

Scalettar, B. A., Swedlow, J. R., Sedat, J. W. and Agard, D. A. (1996). Dispersion, aberration and deconvolution in multi-wavelength fluorescence images. *J. Microsc.* **182**, 50-60.

Schaad, N. C., de Castro, E., Nef, S., Hegi, S., Hinrichsen, R., Martone, M. E., Ellisman, M. H., Sikkink, R., Rusnak, F., Sygush, J. and Nef, P. (1996). Direct modulation of calmodulin targets by the neuronal calcium sensor NCS-1. *Proc. Natl. Acad. Sci. USA* **93**, 9253-9258.

Scheller, R. H. and Hall, Z. W. (1992). Chemical messengers at synapses. In *An Introduction to Molecular Neurobiology* (ed. Z. W. Hall), pp. 119-147. Sunderland, MA: Sinauer Associates.

Steyer, J. A. and Almers, W. (1999). Tracking single secretory granules in live chromaffin cells by evanescent-field fluorescence microscopy. *Biophys. J.* **76**, 2262-2271.

Tooze, S. A. and Huttner, W. B. (1990). Cell-free protein sorting to the regulated and constitutive secretory pathways. *Cell* **60**, 837-847.

Trifaro, J.-M. and Vitale, M. L. (1993). Cytoskeleton dynamics during neurotransmitter release. *Trends Neurosci.* **11**, 466-472.

Tsuboi, T., Zhao, C., Terakawa, S. and Rutter, G. (2000). Simultaneous evanescent wave imaging of insulin vesicle membrane and cargo during a single exocytotic event. *Curr. Biol.* **10**, 1307-1310.

Tsuboi, T., Kikuta, T., Warashina, A. and Terakawa, S. (2001). Protein kinase C-dependent supply of secretory granules to the plasma membrane. *Biochem. Biophys. Res. Commun.* **282**, 621-628.

Werle, M. J., Roder, J. and Jeromin, A. (2000). Expression of frequenin at the frog (Rana) neuromuscular junction, muscle spindle and nerve. *Neurosci. Lett.* **284**, 33-36.

Wiedemann, C., Schafer, T., Burger, M. M. and Sihra, T. S. (1998). An essential role for a small synaptic vesicle-associated phosphatidylinositol 4-kinase in neurotransmitter release. *J. Neurosci.* **18**, 5594-5602.

Zenisek, D., Steyer, J. A. and Almers, W. (2000). Transport, capture and exocytosis of single synaptic vesicles at active zones. *Nature* **406**, 849-854.

Zhao, X., Varnai, P., Tuymetova, G., Balla, A., Toth, Z. E., Oker-Blom, C., Roder, J., Jeromin, A. and Balla, T. (2001). Interaction of neuronal calcium sensor-1 (NCS-1) with phosphatidylinositol 4-kinase beta stimulates lipid kinase activity and affects membrane trafficking in COS-7 cells. *J. Biol. Chem.* **276**, 40183-40189.